2008 Annual Report

Stress Heterogeneity and Its Effect on Seismicity

Principal investigator: James H. Dieterich
Department of Earth Sciences
University of California, Riverside

Introduction

With postdoctoral researcher Deborah Smith a model of seismicity has been developed that integrates 3D stress heterogeneity and rate-state seismicity equations on geometrically complex faults to simulate different parts of the seismic cycle, including aftershock sequences. The model provides physics-based simulations of the temporal and spatial behavior of earthquakes with the characteristic Omori-law decay of aftershock rates as $1/t^p$, and it produces a focal mechanism orientation for each simulated event.

Results

A previously un-modeled feature of aftershocks is the occurrence of aftershocks in "stress shadow" regions where models of Coulomb stress change predict that aftershocks should not occur. Typically there is reduced seismicity, but not a complete absence of aftershocks in stress shadow regions. Indeed, close to the earthquake rupture, aftershocks are usually very intense and are used to map mainshock ruptures. Our simulations indicate that aftershocks in the stress shadow region arise in two ways (Figures 1, 2). First, they can occur close to or on the mainshock fault rupture, because geometric irregularities on the fault generate highly heterogeneous stresses, including localized regions of stress increase within the stress shadow region. Second, in regions away from the fault rupture, some aftershocks occur in the stress shadow region as a consequence of heterogeneous distributions of potential failure planes as defined by heterogeneous initial stress. As a consequence of heterogeneity some faults within the stress shadow zones, which are misaligned with respect to the regional stress, are non-the-less appropriately oriented with respect to the mainshock stress change to generate aftershocks.

Because the simulations employ a heterogeneous population of fault orientations to generate aftershock seismicity, earthquake focal mechanisms can be modeled as well. Of particular interest is the evolution through an aftershock sequence of the statistical parameter β (which is a measure of how well a spatially uniform stress fits a set of earthquake focal mechanisms within a region) and the rotation of the maximum compressive stress, S_H, from stress inversions of focal mechanisms. Modeled changes in β and S_H, comparable to those observed for aftershock sequences, are obtained through adjustment of the parameters controlling the statistics of the heterogeneous fault orientations. However, the simulations indicate that temporal variations of these parameters do not directly correlated with changes in the stress state as generally supposed. This is because seismicity in an aftershock sequence gives a biased sample of changes in stress field. The biasing favors fault orientations that are optimally oriented with respect to stress changes and not total stress. Figure 3 illustrates an example of biasing of focal mechanisms following a mainshock that produces a spurious large apparent rotation of S_H .

Understanding to what degree changes in β and S_H represent actual changes in the Earth's crustal stress is important for earthquake physics. Woessner [2005] used changes in β to estimate temporal evolution of stress heterogeneity during an aftershock sequence. Perhaps even more important, is the use of rotations of observed S_H from stress inversions to estimate the magnitude of crustal stresses. Studies of aftershock seismicity have assumed that rotations of inferred S_H from aftershock stress inversions reflect a "true" rotation of the spatially homogeneous component of the total stress field and can be used to estimate the crustal stress [*Hardebeck*, 2001; *Hardebeck and Hauksson*, 2000; *Hardebeck and Hauksson*, 2001; *Hauksson*, 1994; *Provost and Houston*, 2003; *Woessner*, 2005]. Based on independent estimates of the stress change due to a mainshock, the relatively large apparent rotations of S_H from aftershock focal mechanisms indicate low average crustal stresses ($< 10 MPa$). However, other direct measurements from boreholes suggest much larger crustal stress of the order $\geq 80 MPa$ [*Hickman and Zoback*, 2004; *Townend and Zoback*, 2000; *Townend and Zoback*, 2004; *Zoback and Townend*, 2001; *Zoback, et al.*, 1993]. Our simulations show that large "apparent" rotations of apparent S_H can arise from small stress perturbations using moderate crustal stresses of $50 MPa$; hence, one cannot definitively conclude weak crustal strengths of $< 10 MPa$ from rotations of S_H, where S_H is inferred from stress inversions of aftershock seismicity.

Presentations

Smith, D. and J. Dieterich, *Effect of 3D Stress Heterogeneity on Aftershock Sequences* (Poster), Southern California Earthquake Center, Annual Meeting, Palm Springs, CA, (Sept 9–12, 2008)

Smith, D. and J. Dieterich, *Aftershock Sequences Modeled with 3D Stress Heterogeneity and Rate-State Seismicity Equations: Implications for Crustal Stress*, (Oral Presentation), University of California Los Angeles, Los Angeles, CA, (November 19, 2008).

Smith, D. and J. Dieterich, *Rate-State Seismicity Equations Applied to a 3D Spatially Heterogeneous Stress to Study Aftershock Sequences: Implications for Crustal Stress* (Poster), American Geophysical Union, Fall Annual Meeting, San Francisco, CA, (Dec 15–19, 2008).

Smith, D. and J. Dieterich, *Simulating Stress Relaxation and Aftershock Sequences: Tools for Fault System Modeling and Earthquake Statistics*, (Oral Presentation), United States Geological Survey, Golden, CO, (March 16, 2009).

Smith, D. and J. Dieterich, *Modeling Aftershocks in Spatially Heterogeneous Crustal Stress – How Earthquake Statistics Can Respond to Stress Perturbations,* (Oral Presentation), Jet Propulsion Laboratory, Pasadena, CA, (March 20, 2009).

Paper Accepted by Pure and Applied Geophysics

Aftershock sequences modeled with 3D stress heterogeneity and rate- state seismicity equations: Implications for crustal stress, Smith and Dieterich

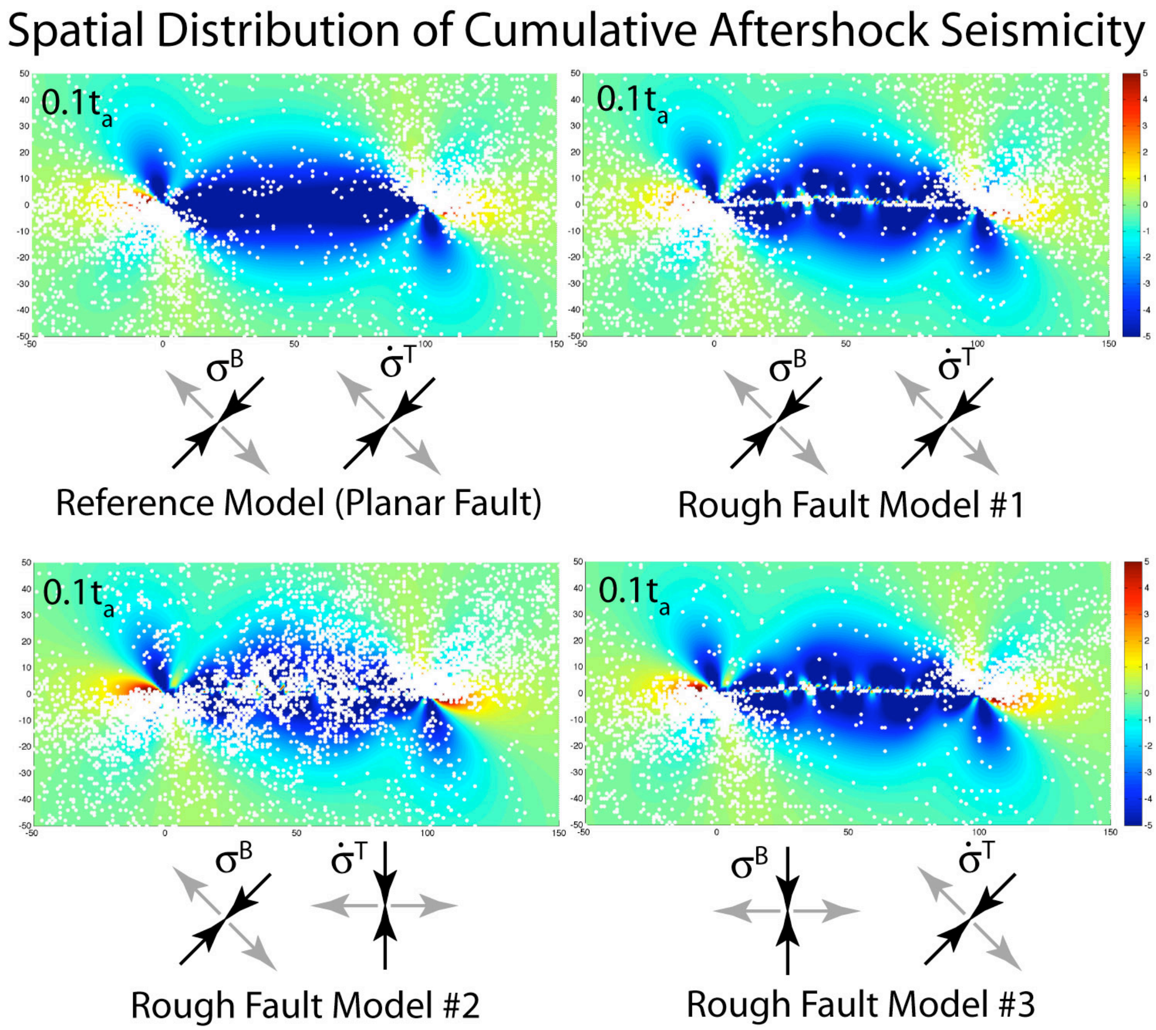

Figure 1. *Simulations of aftershock seismicity resulting from 10m uniform slip on a planar fault (Reference model) and fractally rough faults (models #1, #2, and #3).* $\dot{\boldsymbol{\sigma}}^T$ *and* $\boldsymbol{\sigma}^B$ *are tectonic stressing rate and spatially uniform background stress respectively.* $\dot{\boldsymbol{\sigma}}^T$ *and* $\boldsymbol{\sigma}^B$ *are optimally aligned with respect to the overall fault trend for the Reference model and Rough model #1. The color scale goes from ±5 MPa and the Coulomb stress change is calculated for planes parallel to the planar fault. Each panel shows cumulative aftershock seismicity approximately 0.2-1 years after the mainshock. Note the occurrence of aftershocks within the stress shadow region – these arise from the initial stress heterogeneity, which produces the heterogeneous failure plane population and from stress concentrations along the fractally rough fault.*

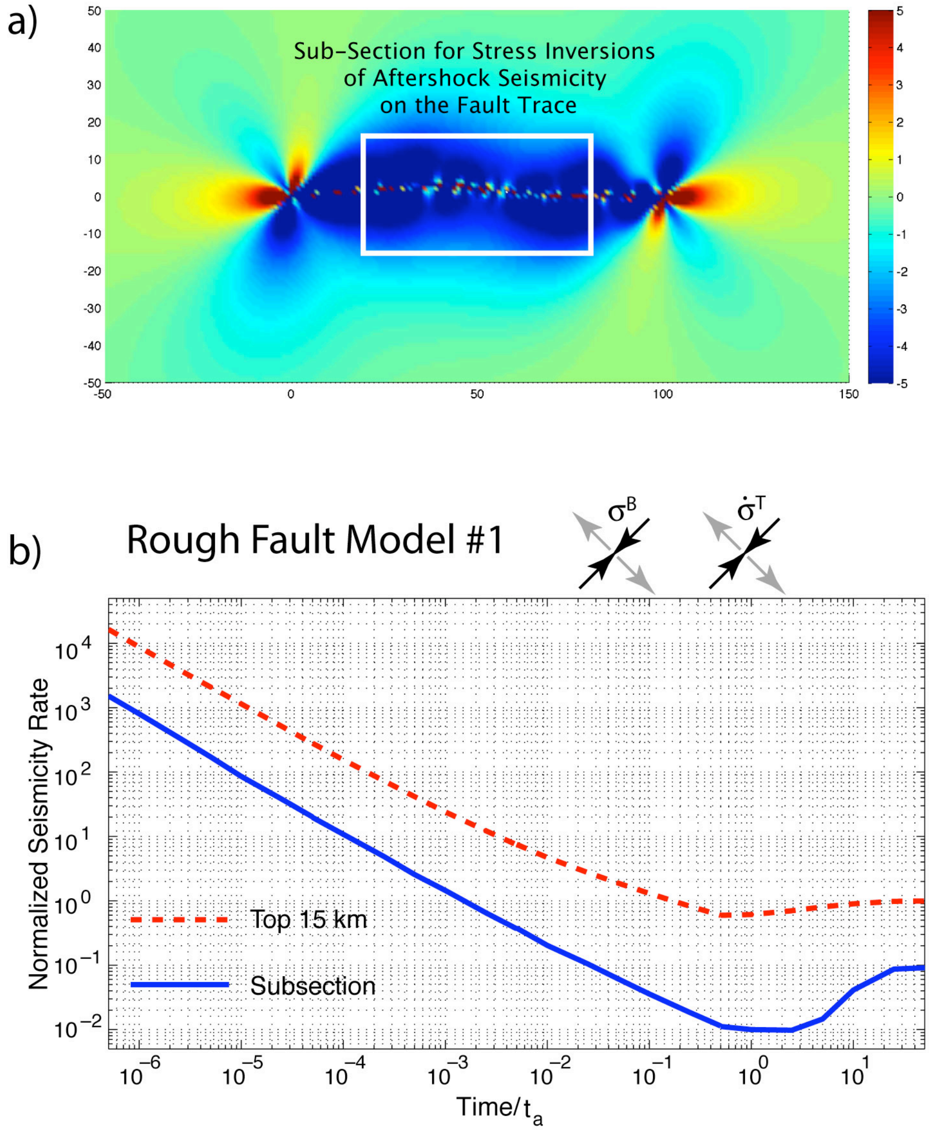

Figure 2. *Normalized seismicity rates as a function of time for the upper 15 km and a subsection close to the fault. In a) the white box delineates the subsection intended to capture seismicity close to or on top of the fault trace similar to aftershock studies. In b) the red dashed line represents seismicity rates calculated for the entire upper 15km of the model region, and the blue solid line represents seismicity rates calculated for the region shown in a). Seismicity rates for both the subsection and entire model region show Omori law like,* $1/t^p$ *behavior with* $p \approx 0.87$. *Note that the rate for the sub-section overshoots its background rate to create a delayed stress shadow then climbs back up at long times.*

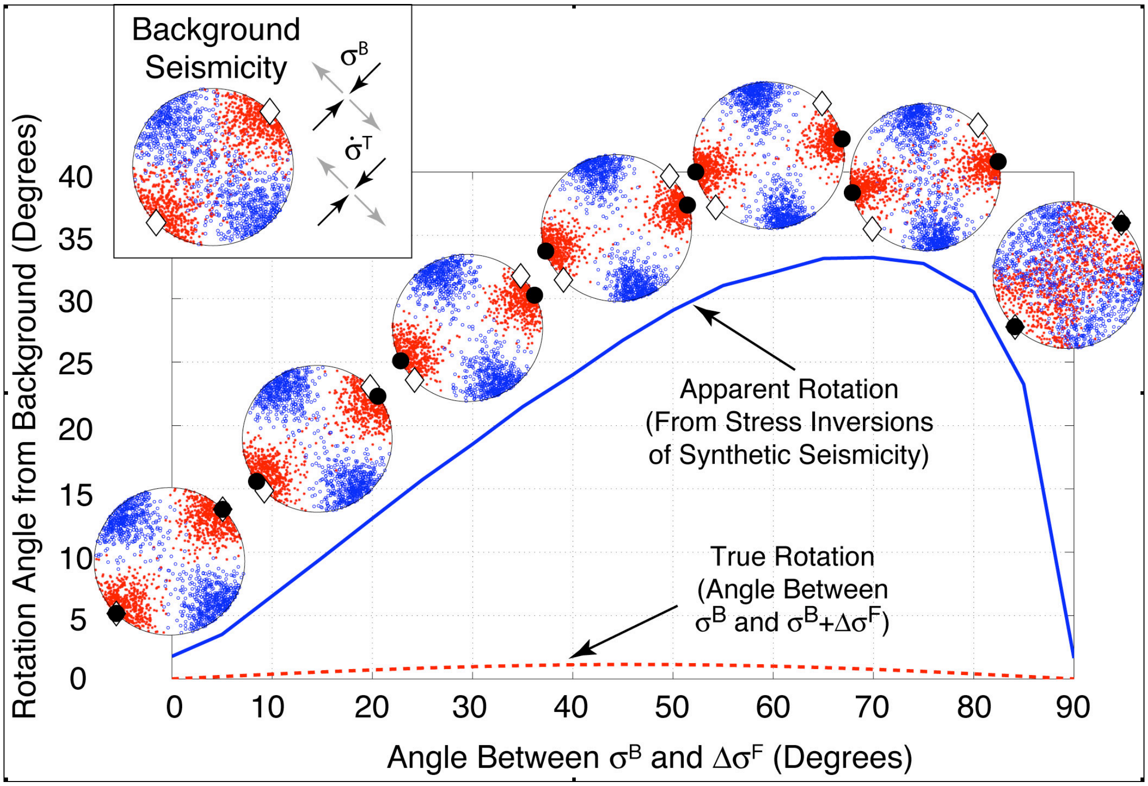

Figure 3. *Plot of "apparent" rotation of the maximum horizontal compressive stress,* S_H*, from inversions of synthetic aftershock seismicity vs. the true rotation from the static stress change,* $\Delta\boldsymbol{\sigma}^F$*.* $\boldsymbol{\sigma}^B$ *is the spatial mean of the initial stress field, and* $\Delta\boldsymbol{\sigma}^F$ *is the static stress change. The principal axes of the stressing rate,* $\dot{\boldsymbol{\sigma}}^T$, are aligned with those of $\boldsymbol{\sigma}^B$. *In this example,* $\Delta\boldsymbol{\sigma}^F$ *is spatially uniform. Aftershock seismicity is evaluated early in the aftershock sequence for various* $\boldsymbol{\sigma}^B$ *and* $\Delta\boldsymbol{\sigma}^F$ *angular differences. The black circles on the plots of synthetic aftershock P-T axes give the orientation of inferred* S_H *for this data, and the open diamonds give* S_H *orientation from the background seismicity prior to the mainshock. The apparent rotation of* S_H*, which is the angular difference between the circles and diamonds is always much larger than the true rotation at every point.*